International Journal of Rock Mechanics & Mining Sciences 48 (2011) 1086–1094

Contents lists available at ScienceDirect

International Journal of Rock Mechanics & Mining Sciences

journal homepage: www.elsevier.com/locate/ijrmms

Prediction of flyrock trajectories for forensic applications using ballistic flight equations

Saša Stojadinović*, Radoje Pantović, Miodrag Žikić

Technical Faculty in Bor, VJ 12, 19 210 Bor, Serbia

ARTICLE INFO

Article history:
Received 1 May 2010
Received in revised form
6 July 2011
Accepted 11 July 2011
Available online 28 July 2011

Keywords:
Flyrock
Ballistic flight
Differential equations
Numeric solution
Runge–Kutta
Trajectories
Safe distance

ABSTRACT

The paper presents a method for determination of the maximum throw of flyrock fragments and the estimation of safe distances. The method is based upon formulation and solution of differential equations of ballistic flight of the flyrock fragments. The equations are formulated according to Newton's law of motion. Two possible solutions are presented, an approximate numerical solution and the application of the Runge–Kutta algorithm of the fourth order. As an illustration of the presented method a post-accidental forensic analysis case study is given describing the procedure for determination of the input parameters (especially the launch velocity).

1. Introduction

Despite the advance in blasting and explosives technologies, adverse effects of blasting still remain an issue in both surface and underground blasting operations. While seismic effects of blasting affect only the surrounding structures and can cause material damage, flyrock affects machinery, structures and people. Since flyrock can cause severe injuries to people, even fatal, it is the biggest blasting safety concern.

Flyrock is commonly a result of a mismatch between the energy applied and the energy needed for rock fragmentation and casting. This mismatch is the result of technical and natural factors such as blasthole deviation, insufficient burden, insufficient stemming, existence of faulted or weakened zones in the rock, etc. While technical factors can be controlled through precision drilling and control of blasting pattern and geometry, natural factors usually cannot be influenced.

There are generally three flyrock mechanisms, cratering, rifling and face burst, which are defined upon the origin of the flyrock fragments. Cratering is the result of insufficient stemming height so that flyrock comes from the crater formed around the blasthole collar. Rifling is a result of insufficient or absent stemming so that stemming material or rock fragments are propelled through the blasthole upwards. Face burst is a result of weakened and faulted zones in the bench face. The detonation products follow the line of the least resistance i.e. weakened zone, propelling the rock fragments from the bench face.

Safety concerns regarding flyrock result in the establishment of safe distances for machinery and people determined by the maximum throw of the flyrock fragments multiplied by some safety factor.

A number of studies [1–3] suggest the scaled burden approach for the flyrock range prediction and hence the safe distance definition. All this applies to "normal" flyrock. In some rare cases, due to a combination of various factors or an error in the blast design a "wild" flyrock, flyrock traveling distances far beyond the safe distance, can occur. These excess cases require forensic analysis of the event in order to determine the cause of flyrock and usually result in the redefinition of the safe distances.

Various approaches can be used to redefine the safe distance but this paper suggests the formulation and solution of differential equations of ballistic flight of the flyrock fragments.

2. Physics of the flyrock fragment flight

The first step in the overall solution is the analysis of the forces acting upon the flyrock fragment and the application of the second Newton's law of motion. The basic forces acting upon the flyrock fragment following the trajectory or the path ***s***, at any

* Corresponding author. Tel.: +381 60 4807819; fax: +381 30 421078.
E-mail addresses: sstojadinovic@tf.bor.ac.rs (S. Stojadinović), pan@tf.bor.ac.rs (R. Pantović), mzikic@tf.bor.ac.rs (M. Žikić).

1365-1609/$ - see front matter © 2011 Elsevier Ltd. All rights reserved.
doi:10.1016/j.ijrmms.2011.07.004

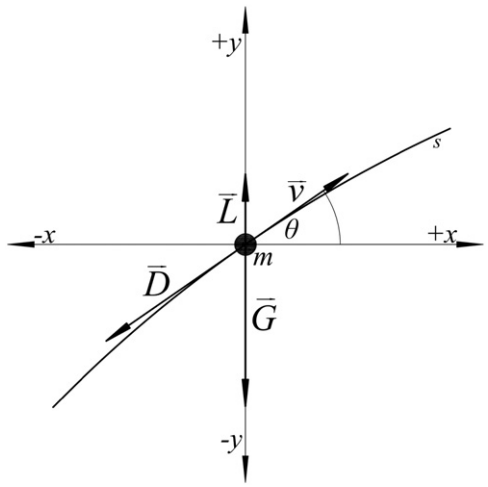

Fig. 1. Basic forces acting upon the flyrock fragment.

moment of flight, are the gravity force (***G***), the resistance force or drag (***D***) and the force of lift (***L***) (Fig. 1).

In some cases, the ballistic flight equations could include additional forces such as wind influence or the Coriolis effect (inertial force as a result of the Earth's rotation) [4–6] but in the case of flyrock these influence can be neglected. The influence of wind should be considered if the flyrock fragment has a small mass and the Coriolis effect can be expected at altitudes that flyrock fragments cannot reach.

During flight, at any moment of time, according to the second Newton's law of motion, an equilibrium condition can be defined by the vector equation

$$\boldsymbol{F} = m\boldsymbol{a} = \boldsymbol{G} + \boldsymbol{D}, \tag{1}$$

or

$$m\boldsymbol{a} = \boldsymbol{G} + \boldsymbol{D} + \boldsymbol{L}, \tag{2}$$

where $\boldsymbol{a}$ is the acceleration of the system. Gravitational force, drag and lift are defined as follows:

$$\boldsymbol{G} = m\boldsymbol{g}, \tag{3}$$

$$\boldsymbol{D} = \frac{1}{2}\rho A C_D v^2 = C_1 v^2, \tag{4}$$

$$\boldsymbol{L} = \frac{1}{2}\rho A C_D v_f^2 = C_2 v_f^2, \tag{5}$$

where m is the mass of the flyrock fragment (kg), $\boldsymbol{g}$ is the gravitational acceleration (m/s^2), ρ is the density of air (kg/m^3), A is the cross-sectional area of the flyrock fragment, along a plane perpendicular to the direction of flight (m^2), C_D is the dimensionless drag coefficient, v is the flyrock fragment velocity (m/s), C_L is the dimensionless lift coefficient and v_f is the free-stream velocity (m/s). Due to its small, value the lift force can be neglected.

Eq. (2) is the starting point for the formulation of the differential equations of ballistic flight of the flyrock fragments. The final solution is the set of data pairs (x, y) defining the trajectory and hence the throw of a flyrock fragment. This paper suggests two possible approaches for the formulation and solution of the differential equations, an approximate numerical solution and the Runge–Kutta algorithm solution.

3. Formulation and solution of differential equations

3.1. An approximate numerical solution

If projected to horizontal (x) and vertical (y) axis (Fig. 2), Eq. (2) can be written as a system of two differential equations

$$\begin{aligned} m\ddot{x} &= -D_x = -C_1 v^2 \cos\theta \\ m\ddot{y} &= -mg - D_y = -mg - C_1 v^2 \sin\theta, \end{aligned} \tag{6}$$

where $\ddot{x}$ is the horizontal component of the system acceleration (m/s^2), $\ddot{y}$ is the vertical component of the system acceleration (m/s^2) and θ is the angle between the velocity vector (tangent) and the horizontal axis (degree). Since the angle θ is time dependent, the sine and cosine functions are defined as

$$\begin{aligned} v_y &= v\sin\theta \Rightarrow \sin\theta = \frac{v_y}{v} \\ v_x &= v\cos\theta \Rightarrow \cos\theta = \frac{v_x}{v}, \end{aligned} \tag{7}$$

where v_x and v_y are horizontal and vertical component of the velocity, respectively.

For the initial conditions $t=0 \rightarrow x=x_0$, $y=y_0$, $v=v_0$ and $\theta=\theta_0$ (where v_0, θ_0 are the launch velocity and angle, respectively) the system of Eq. (6) can be written as

$$\begin{aligned} \ddot{x}_0 &= -\frac{1}{m} C_1 v_0^2 \frac{v_{x0}}{v_0} \\ \ddot{y}_0 &= -g - \frac{1}{m} C_1 v_0^2 \frac{v_{y0}}{v_0}, \end{aligned} \tag{8}$$

At any moment of the flyrock fragment flight the parameters of flight can be calculated as

$$\begin{aligned} v_{x(i+1)} &= v_{x(i)} + \ddot{x}_{(i)}\Delta t \\ v_{y(i+1)} &= v_{y(i)} + \ddot{y}_{(i)}\Delta t, \end{aligned} \tag{9}$$

$$V_{(i+1)} = \sqrt{v_{x(i)}^2 + v_{y(i)}^2}, \tag{10}$$

$$\begin{aligned} \ddot{x}_{(i+1)} &= -\frac{1}{m} C_1 v_{(i)}^2 \frac{v_{x(i)}}{v_{(i)}} \\ \ddot{y}_{(i+1)} &= -g - \frac{1}{m} C_1 v_{(i)}^2 \frac{v_{y(i)}}{v_{(i)}}, \end{aligned} \tag{11}$$

and finally,

$$x_{(i+1)} = x_{(i)} + v_{x(i)}\Delta t + \frac{\ddot{x}_{(i)}\Delta t^2}{2}$$

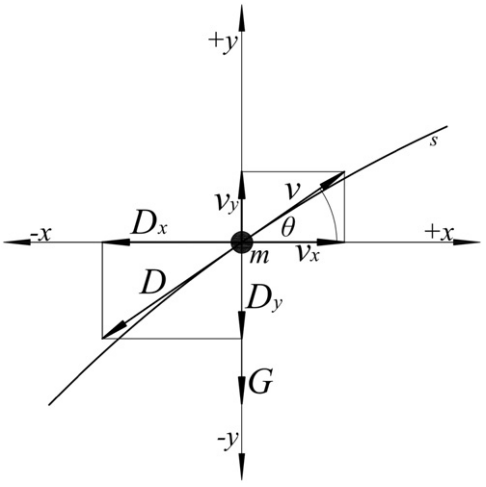

Fig. 2. Horizontal and vertical projections of the velocity and the drag.

$$y_{(i+1)} = y_{(i)} + v_{y(i)}\Delta t + \frac{\ddot{y}_{(i)}\Delta t^2}{2}, \tag{12}$$

where Δt is the timestep.

The set of Eq. (12) gives the coordinates of the flyrock fragment at discrete moments of flight (x, y). The graphical representation of these data pairs is the trajectory of the flyrock fragment. The maximum flyrock throw x_{max} is determined from the condition $y=0$ (fragment hits the ground).

3.2. Application of the Runge–Kutta algorithm

In this case Eq. (2) is projected on the directions of normal and tangent to the trajectory (Fig. 3) and can be written as

$$\begin{aligned} ma_\tau &= -G_\tau - D = -mg\sin\theta - C_1 v^2 \\ ma_n &= -G_n = -mg\cos\theta, \end{aligned} \tag{13}$$

where a_τ and a_n are tangential and normal component of the acceleration, respectively.

At any moment of flight the flyrock fragment follows the path s. The path s can be considered as a curve that consists of a series of circular arcs with corresponding radii R_C. The property of the curved path s is the curvature k. From the differential geometry the curvature can be expressed as [7,8]

$$k = \frac{d\theta}{ds}, \tag{14}$$

But also as

$$k = \frac{1}{R_C}, \tag{15}$$

Hence

$$\frac{1}{R_C} = \frac{d\theta}{ds}. \tag{16}$$

According to the definition of the velocity as the first derivative of the path over time the velocity can be expressed as

$$v = \frac{ds}{dt}. \tag{17}$$

From the basic dynamics, tangential and normal (radial) acceleration are

$$a_\tau = \frac{dv}{dt} \text{ and } a_n = \frac{v^2}{R_c}. \tag{18}$$

With velocity vector projected to horizontal and vertical axis, using the relations $a_t = dv/dt$ and $a_n = v^2/R_c$, where $1/R_c = d\theta/ds$,

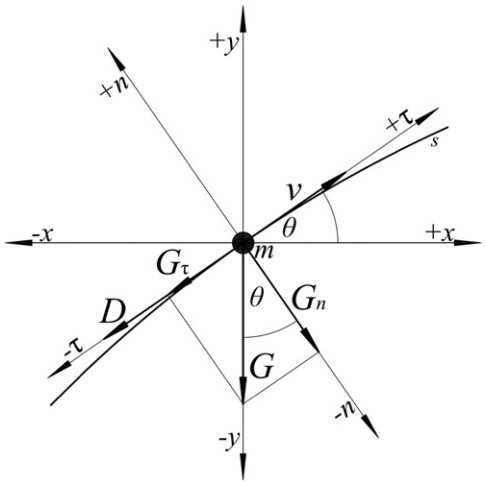

Fig. 3. Tangential and normal components of the forces acting upon the flyrock fragment.

and with $v = ds/dt$, the set of Eq. (13) can be rewritten as

$$\begin{aligned} \frac{dv}{dt} &= -g\sin\theta - \frac{C_1}{m}v^2 = -g\sin\theta - Cv^2 \\ \frac{d\theta}{dt} &= -\frac{g\cos\theta}{v} \\ \frac{dx}{dt} &= v\cos\theta \\ \frac{dy}{dt} &= v\sin\theta. \end{aligned} \tag{19}$$

The set of Eq. (19) is the system of differential equations, which can be solved using the Runge–Kutta algorithm of the fourth order (RK 4) in the form [9,10]

$$\begin{aligned} v_{i+1} &= v_i + \frac{h}{6}(f_1 + 2f_2 + 2f_3 + f_4) \\ \theta_{i+1} &= \theta_i + \frac{h}{6}(g_1 + 2g_2 + 2g_3 + g_4), \end{aligned} \tag{20}$$

where h is the timestep and

$$\begin{aligned} \tfrac{dv}{dt} &= f(t_i, v_i, \theta_i) & \tfrac{d\theta}{dt} &= g(t_i, v_i, \theta_i) \\ f_1 &= f(t_i, v_i, \theta_i) & g_1 &= g(t_i, v_i, \theta_i) \\ f_2 &= f\left(t_i + \tfrac{h}{2}, v_i + \tfrac{h}{2}f_1, \theta_i + \tfrac{h}{2}g_1\right) & g_2 &= g\left(t_i + \tfrac{h}{2}, v_i + \tfrac{h}{2}f_1, \theta_i + \tfrac{h}{2}g_1\right), \\ f_3 &= f\left(t_i + \tfrac{h}{2}, v_i + \tfrac{h}{2}f_2, \theta_i + \tfrac{h}{2}g_2\right) & g_3 &= g\left(t_i + \tfrac{h}{2}, v_i + \tfrac{h}{2}f_2, \theta_i + \tfrac{h}{2}g_2\right) \\ f_4 &= f(t_i + h, v_i + hf_3, \theta_i + hg_3) & g_4 &= g(t_i + h, v_i + hf_3, \theta_i + hg_3) \end{aligned} \tag{21}$$

and

$$\begin{aligned} x_{i+1} &= x_i + \frac{h}{6}(p_1 + 2p_2 + 2p_3 + p_4) \\ y_{i+1} &= y_i + \frac{h}{6}(q_1 + 2q_2 + 2q_3 + q_4), \end{aligned} \tag{22}$$

where

$$\begin{aligned} \tfrac{dx}{dt} &= p(t_i, v_i, \theta_i) & \tfrac{dy}{dt} &= q(t_i, v_i, \theta_i) \\ p_1 &= f(t_i, v_i, \theta_i) & q_1 &= f(t_i, v_i, \theta_i) \\ p_2 &= f\left(t_i + \tfrac{h}{2}, v_i + \tfrac{h}{2}f_1, \theta_i + \tfrac{h}{2}g_1\right) & q_2 &= f\left(t_i + \tfrac{h}{2}, v_i + \tfrac{h}{2}f_1, \theta_i + \tfrac{h}{2}g_1\right). \\ p_3 &= f\left(t_i + \tfrac{h}{2}, v_i + \tfrac{h}{2}f_2, \theta_i + \tfrac{h}{2}g_2\right) & q_3 &= f\left(t_i + \tfrac{h}{2}, v_i + \tfrac{h}{2}f_2, \theta_i + \tfrac{h}{2}g_2\right) \\ p_4 &= f(t_i + h, v_i + hf_3, \theta_i + hg_3) & q_4 &= f(t_i + h, v_i + hf_3, \theta_i + hg_3) \end{aligned} \tag{23}$$

The set of Eq. (22) gives the coordinates of the flyrock fragment at discrete moments of flight and hence the trajectory.

4. A case study

Kamenica quarry is located some 13 km south of Kraljevo, central Serbia. On May 5th 2007, blasting operations at the quarry resulted in massive wild flyrock. Fortunately, no one was injured but several surrounding structures were hit by the flyrock fragments and severely damaged. The authors of this paper were engaged in conducting a forensic investigation in order to determine the causes of the flyrock. The procedure of the numerical solution to the flyrock differential equations of motion and trajectory prediction is given by an example of the Kamenica andesite quarry.

4.1. The analysis of the flyrock event

The Kamenica andesite quarry has an elevated position in relation to the main stone processing platform and the surrounding area. It is located near the top of a hill at an elevation of 430 m above sea level. The material from the quarry is gravitationally transported to the main platform down a 100 m high cliff (Fig. 4). The blasting site on May 5th consisted of five individual blasting series (Fig. 4) with a total of 122 76-mm-diameter blastholes.

The drilling pattern was staggered with designed burden $B=2.8$ m and spacing $S=3.0$ m and blastholes were parallel to the bench face. The bench height was 14 m and the angle was 70°. The blasthole length varied from 3 m (series I) to 15.5 m (series II). Two types of cartridged explosives were used, Emulgit 82GP 60/2000 and Emex AN 65/2500 with a total amount of 4467 kg. The characteristics of the used explosives are given in Table 1. 130 non-electric detonators with 17/500 surface/blastohole delay were used for the initiation of the blasting series. The maximum charge per delay was 63.5 kg [11].

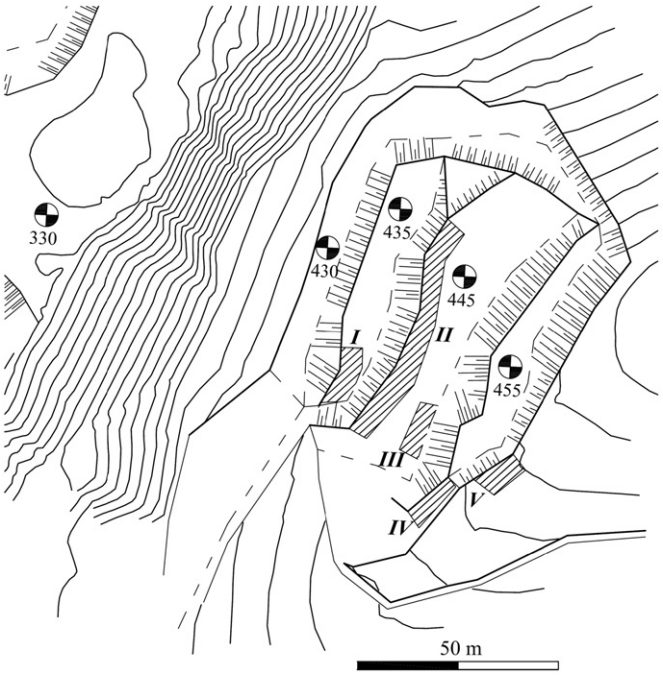

Fig. 4. Topography of the quarry and the position of the blasting series I–V.

Table 1
The characteristics of the applied explosives.

Characteristic	Symbol	Unit	Value	
			Emulgit 82GP	Emex AN
Density	ρ_E	g/cm^3	1.2	1.2
Volume of products	V	dm^3/kg	868	1011
Specific energy	q	kJ/kg	911	861
Detonation velocity	D	m/s	4100	4700
Oxygen balance	O_2	%	−1.4	−3.5
Heat of explosion	Q	kJ/kg	4058	3040
Cartridge diameter	d_C	mm	60	65
Cartridge mass	m_C	kg	2.0	2.5
Cartridge length	l_C	m	0.59	0.63

The investigation revealed that face burst was the basic mechanism of flyrock in this case. This was supported by the fact that there were blastholes with intact or almost intact stemming zone (Fig. 5).

The flyrock came from the whole blasting field but the main bursting zone was the central part of the blasting series II and series V.

The final conclusion of the analysis was that the cause of the flyrock was an unfortunate combination of natural and technical factors. The rock mass in the bursting zone was highly faulted and hence weakened. The presence of alternate zones of firm (compact) and altered (weak) andesite additionally complicated the conditions. The faulting and the alterations (different shades of gray) of the rock mass can be noticed in Fig. 5. Although the designed burden should have been 2.8 m, the actual burden in some parts of the blasting series II was only 0.7 – 1.2 m (Fig. 6). Drillhole deviation was not monitored and it probably contributed to the flyrock occurrence.

Since several surrounding structures were hit by the flyrock fragments and damaged, it was necessary to inspect the surrounding area. The main reasons for the inspection were to

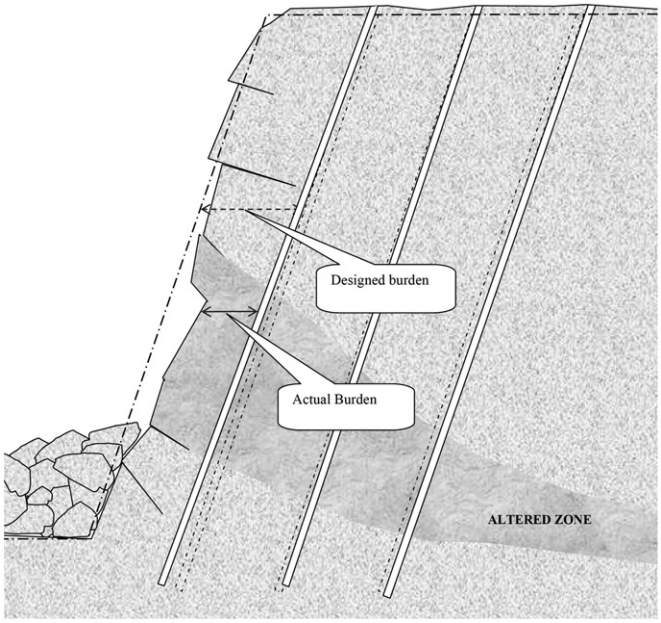

Fig. 6. Cross-section through the blasting series II showing causes of flyrock.

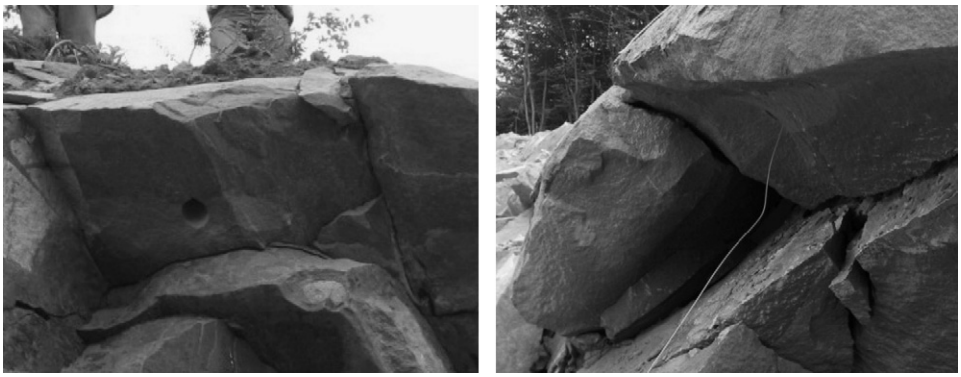

Fig. 5. Intact stemming zones indicating face burst flyrock mechanism.

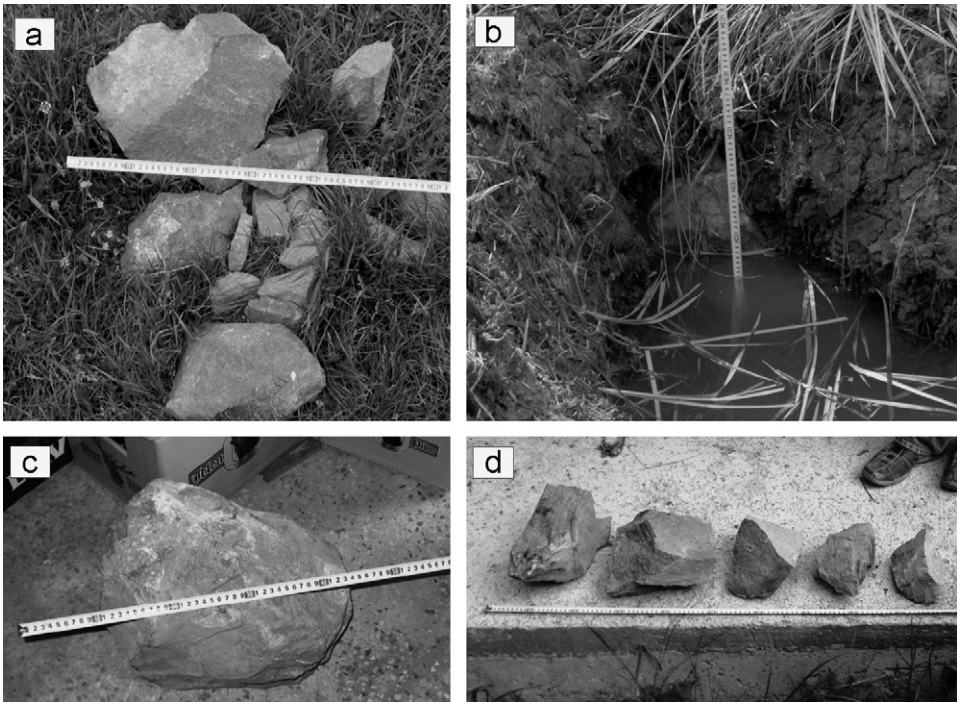

Fig. 7. Flyrock fragments found in the area from Fig. 8 (measuring tape in cm). Various sizes position d (a), crater in the soft soil position c (b), position f (c) and position a (d).

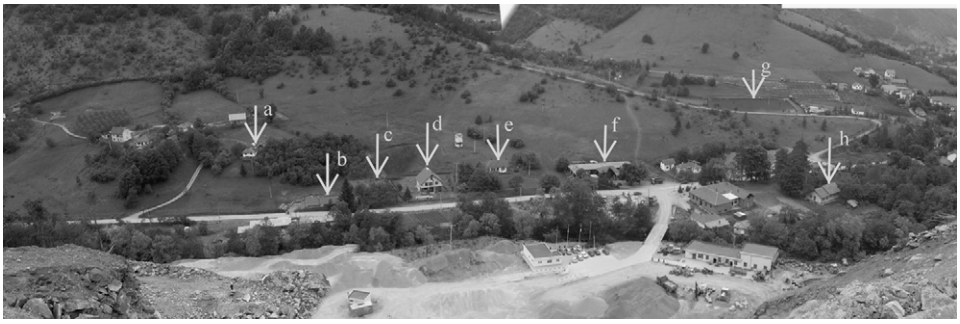

Fig. 8. Panoramic view of the affected structures and the impact area (Photos taken from the quarry bench and photomerged) Family house (a), saw mill (b), fragment crater (c), family house (d), family house (e), tavern (f), fish pond (g) and primary school (h).

determine the size of the flyrock fragments, their number, the severity of damage to structures and determine the affected area in order to redefine the safe distance. The inspection revealed that flyrock fragments had sizes varying from 3–50 cm and more in diameter and that, on average, there was one fragment per 16 m^2 (Fig. 7)

The most severely damaged structure was a two story family house with several flyrock fragments penetrating trough the roof and walls (Fig. 8 position d and Fig. 9).

However, it was impossible to inspect the whole area and determine the affected zone in that way. Consequently, an attempt was made to formulate the differential equations of ballistic flight of the flyrock fragments. The basic idea was that solutions of these equations would give the trajectories and maximum throw of the flyrock fragments and hence determine the affected area and define the safe distance.

4.2. Formulation and solution to differential equations

The differential equations were formulated as described previously (Eqs. (1–5)) and solved using an approximate numerical solution and the RK 4 method. The differential equations were formulated and solved for flyrock fragments of sizes 5, 10, 15, 20, 25, 30, 35, 40, 45 and 50 cm in diameter. The basic input parameters to the differential equations were the mass of the flyrock fragments, the launch angle and the launch velocities. The flyrock fragments were approximated as spheres with the diameter corresponding to an average dimension of the fragment.

The mass of the fragment was calculated as

$$m = \frac{4}{3}\left(\frac{d}{2}\right)^3 \pi \rho_R, \tag{24}$$

where d is the fragment size (m), and ρ_r density of the rock (2600 kg/m^3). The launch angle was assumed to be 45° and this decision was supported by the fault dip of approximately the same value (Fig. 5) and the fact that 45° angle should give maximum throw. The launch velocity, as one of the main parameters, was difficult to estimate. Some literature sources [3] suggest the estimation of the launch velocity using an impulse approach

$$v_0 = \frac{3\rho_E D^2 \Delta t}{32 d \rho_R}, \tag{25}$$

where Δt is the length of impulse time (1.8×10^{-6} s) [3].

Fig. 9. The damage to structure (50 cm flyrock fragment at 320 m distance).

If applied, this equation results in the launch velocity of less than 3.5 m/s for a 50 cm fragment and gives the maximum throw of less than 10 m. On the other hand, fragments of this size were found at distances of 300 m and more. This indicated that, if applicable, Eq. (25) would give the launch velocities for "normal" flyrock or was highly case specific and that different approach was needed.

The solution which was not case specific was ballistic approach. With the known actual throw and mass of the flyrock fragments, it was possible to formulate and analytically solve the differential equations of ballistic flight neglecting the drag and lift. With the "no atmosphere" condition the vector Eq. (2) becomes

$$m\boldsymbol{a} = \boldsymbol{G}, \tag{26}$$

and the set of Eq. (6) becomes

$$m\ddot{x} = m\frac{d^2x}{dt^2} = 0$$
$$m\ddot{y} = m\frac{d^2y}{dt^2} = -mg \tag{27}$$

Integration of these differential equations gives the expressions for x and y coordinates of flyrock fragment at any moment of time as

$$x = x_0 + v_0 t\cos\theta, \tag{28}$$

$$y = y_0 + v_0 t\sin\theta - \frac{gt^2}{2}. \tag{29}$$

If t is expressed from Eq. (28), for the initial condition that $x_0=0$,

$$t = \frac{x}{v_0\cos\theta}, \tag{30}$$

and replaced in Eq. (29) (for the condition that for $t=t_{max}y=0$), the launch velocity can be expressed as

$$v_0 = x\sqrt{\frac{g}{2y_0\cos^2\theta + 2x\sin\theta\cos\theta}}. \tag{31}$$

If Eq. (25) is analyzed, a conclusion can be made that the largest fragments have the lowest launch velocities. Since the largest flyrock fragments were 50 cm, and were not found at distances larger than 320 m, this fragment size was used to calculate the minimal launch velocity. For the initial conditions $x_0=0$, y_0 =100 m, x=320 m, according to Eq. (31) the launch velocity of the 50 cm fragments was 47 m/s. Since the drag force was neglected during these calculations the actual launch velocity should be estimated by increasing the calculated velocity by 15–20%. This way the launch velocity of the largest flyrock fragments was set to 55 m/s. Considering the conclusion that smaller fragments have higher launch velocities, an attempt was made to estimate the launch velocity of the smallest fragment by modifying Eq. (25) into

$$v_0 = C_f\frac{3\rho_E D^2\Delta t}{32d\rho_R}, \tag{32}$$

where C_f would be a correction factor, which should adjust Eq. (25) to specific conditions of the study. The first step in the estimation of the launch velocity of the smallest fragments was the calculation of C_f. Since launch velocity of the largest fragment was estimated using ballistic approach, C_f was calculated from the data for the largest fragment by transformation of Eq. (32)

$$C_f = v_0\frac{32d\rho_R}{3\rho_E D^2\Delta t}. \tag{33}$$

For the values of detonation velocity and density of Emex AN (Table 1, Section 4) and 50 cm fragment launch velocity of 55 m/s, Eq. (33) yields the correction factor C_f=16. Applying this value to calculate the velocity of the smallest fragment, Eq. (32) gives the launch velocity of the 5 cm fragment v_0=550 m/s. This was an extremely high value and it became obvious that this approach was erroneous. This confirmed the first conclusion that Eq. (25) is case specific and should be used with caution and reserve.

On the other hand, there was no data solid enough to base the calculations upon. In the case of the 50 cm fragments, the fact was that fragments did not fall at distances larger than 320 m. The majority of the 5 cm fragments fell at distances below 300 m but it was not possible to claim with certainty that this was their maximum throw. Because of that, the launch velocity of the 5 cm fragment was also estimated using ballistic approach. Since the recorded throw of the smallest fragments was 300–350 m, the launch velocity of the 5 cm fragments was estimated using ballistic equations (no drag) and set to 150 m/s, which corresponds to the recorded throw. The launch velocities for the other fragment sizes were considered to be between these two values (55 and 150 m/s) and were estimated and set as shown in Table 2. It must be mentioned that estimation of the velocities for the fragments between 5 and 50 cm was not supported by any calculations. The reason for that was the fact that it was impossible to inspect the whole area affected by flyrock to determine the maximum throw for each fragment size and the purpose of the formulation of ballistic equations was to estimate the unknown throws.

In the current work, fragments have been approximated to spheres. The drag coefficient C_D for spheres is in the range of 0.07–0.5 [12]. However, in this case the drag coefficient was

Table 2
The initial parameters of flyrock fragments.

Particle size (m)	Launch velocity (m/s)	Mass (kg)	Cross-section area (m^2)
0.05	150	0.2	0.002
0.10	140	1.4	0.008
0.15	130	4.6	0.018
0.20	120	10.9	0.031
0.25	105	21.3	0.049
0.30	90	36.7	0.071
0.35	80	58.3	0.096
0.40	70	87.1	0.126
0.45	60	124.0	0.159
0.50	55	170.1	0.196

chosen to be 0.8 to compensate for the irregularity and the surface roughness of the fragments.

4.3. The trajectories of the flyrock fragments

The trajectories of the flyrock fragments were calculated and plotted according to the approximate numerical solution and RK 4 algorithm. The input parameters for calculations were as follows. Fragment size $d=5$–50 cm, launch velocity (see Table 2), launch angle $\theta=45^{\circ}$, Fragment mass (see Table 2), fragment cross-sectional area (see Table 2), Drag coefficient $C_D=0.8$, air density $\rho=1.2044$ kg/m^3 and timestep $\Delta t=0.2$ s.

The trajectories of the flyrock fragments are given in Figs. 10 and 11 and the impact zone (the area affected by flyrock) is given in Fig. 12. The impact zone was defined by the maximum throws and the topography of the terrain.

It is interesting to notice that the largest throw was not recorded for the smallest fragments, which were assumed to have the highest launch velocity. The largest throw was recorded for the mid-sized fragments. Any attempt of explanation of these, to some extent illogical, results must consider the initial forces, which are propelling the fragments as well as the forces acting upon fragments during flight.

In order to discuss the initial propelling forces several assumptions must be made. The first assumption is that the fragments are propelled by the pressure of gaseous products of detonation. Further, it is assumed that the gaseous products of detonation take the form of an ellipsoidal bubble and the pressure is equal in

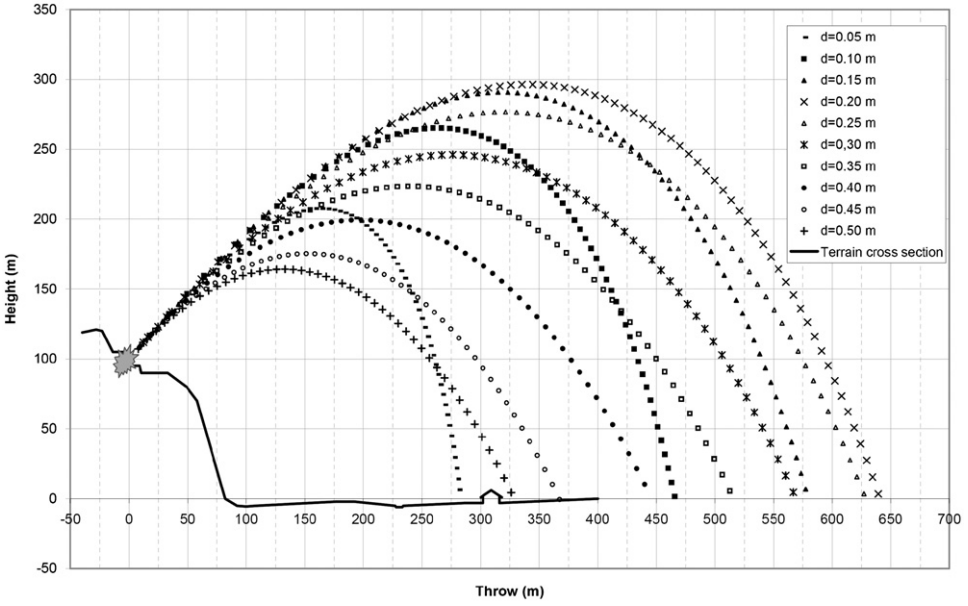

Fig. 10. Trajectories plotted according to an approximate numerical solution.

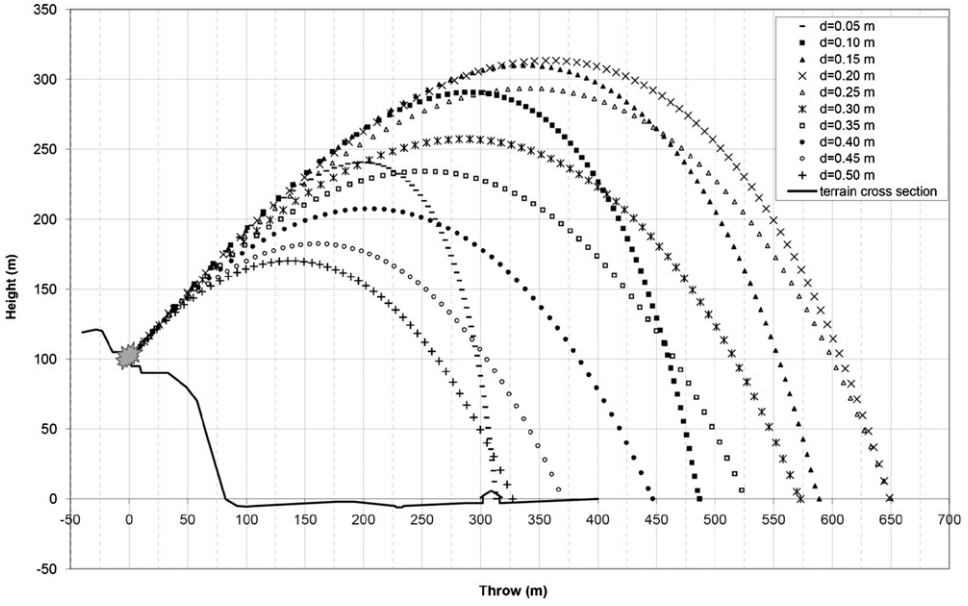

Fig. 11. Trajectories plotted according to RK 4 solution.

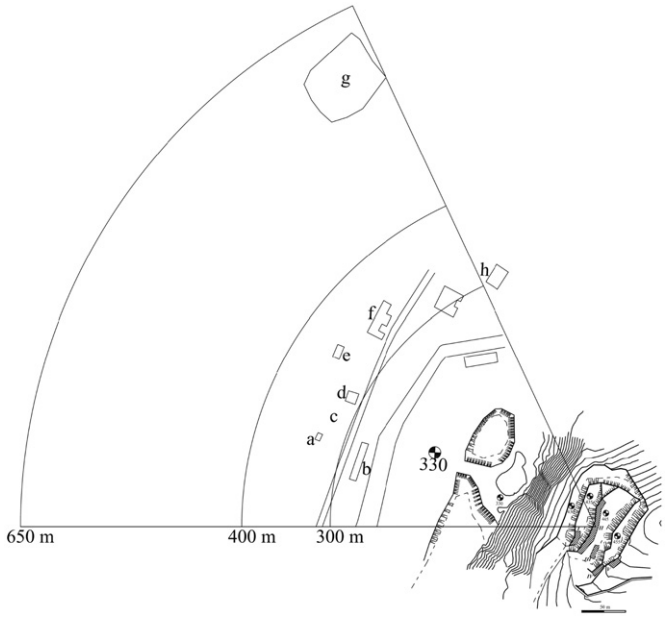

Fig. 12. Maximal throw of the flyrock fragments and the impact zone (positions the same as in Fig. 8).

nearby points of the bubble surface. This leads to the conclusion that nearby fragments, regardless of their size, are affected by the same pressure. The force acting upon a fragment depends on the amount of pressure and the area of the fragment. The smaller the area of the fragment the smaller the force and hence the velocity of the fragment is lower. On the other hand, the force resisting the movement is the inertia of the fragment. Inertial force is directly dependent on the mass of the fragment. Again, a smaller fragment has smaller mass resulting in a smaller inertial force and hence higher velocity. The conclusion is that the launch velocity depends on the ratio of the propelling and inertial forces. Now, looking at Table 2 and comparing the 5 and 50 cm fragments it can be seen that the 50 cm fragment has a 100 times larger cross-sectional area than the 5 cm fragment (resulting in a 100 times larger propelling force). The 50 cm fragment, however, has a 1000 times larger mass than the 5 cm fragment (resulting in 1000 times larger inertial forces). The overall ratio of propelling and inertial forces for the 5 and 50 cm fragments is 10 times in favor of the 5 cm fragment confirming the assumption that smaller fragments have higher launch velocities.

Once airborne the fragments maximum throw is affected by the horizontal component of the resistance forces. Looking at Eqs. (4) and (6) it is obvious that the acceleration of the fragment depends upon the drag force and mass of the fragment. Drag force is dependent upon the cross-sectional area of the fragment and the velocity squared. The acceleration, however, is inversely dependent upon mass again due to the inertia of the fragment. Now, comparing the two fragments of different sizes (5 and 50 cm) the following can be concluded.

Although the smaller fragment has smaller cross-sectional area the higher launch and flight velocities result in larger drag forces. Unlike the larger fragment, the small fragment has a small mass (inertia), which is insufficient to overcome the drag forces. The drag forces are therefore dominant preventing the fragment to reach large throws. However, the inertia of the larger fragment is large enough to be a dominant force since, despite larger cross-sectional area, low launch and flight velocities result in a smaller drag force. The inertia is then the governing force allowing the larger fragments to reach some larger throws.

The differences in throws of various fragment sizes presented in Figs. 10 and 11 are the result of a balance in drag forces and inertia of the flying fragments. The propelling and resistance forces acting upon the midsize fragments are balanced in a way that allows them to reach maximum throws. As can be seen from the figures, the maximum throw of flyrock fragments during blasting at Kamenica quarry on May 5th 2007 was 650 m for the 20 and 25 cm fragments. This corresponds to the statements of some eye witnesses that flyrock fragments were falling into a nearby fish pond at the distance of more than 500 m.

These results led to the conclusion that it was necessary to set the safe distance for residents at distances larger than 700 m. However, considering the fact that this was an excess case, the probability of reappearance is low but existent. Considering that, efforts should be made to calculate the risk of flyrock of this magnitude and define the risk zones (zones with specific probability/risk of flyrock impact) within the recorded zone of impact. It is obvious that during each new blast at the quarry, the residents from the nearest structures should be evacuated and that the residents from the other structures (within the 700 m distance) should be alerted. The proximity of the school (within the 400 m distance) should be taken into account and the blasts, without exceptions, must be performed on a no school day or after school hours. Considering the low frequency of the blasts (up to two blasts a month) this solution (evacuation and no school limitation) is feasible. An alternative is relocation of several closest structures but having in mind the frequency of the blasts and the probability of incident reappearance this alternative is not cost-effective.

5. Conclusions

The basic conclusion of this paper is that it is possible to formulate the differential equations of ballistic flight of flyrock fragment and use these equations to calculate/determine/estimate the maximum throw. The solution of the differential equations can be obtained using an approximate numerical approach or the Runge–Kutta algorithm of the fourth order. However, a remark must be made that *this solution requires input data* (*throw and mass for velocity back calculations*) *that are available only after the incident*. This means that this approach is more suitable for post-accidental analysis of the flyrock event and redefinition of the safe distances since enough data exists to support the calculations. It can be certainly used to estimate the safe distances at a new site upon similar experiences but only in early phases of operation and with high reserve.

This approach is also suitable for urban blasting where flyrock presents a serious threat to the surrounding structures. A remark must be made on the absence of proper method for launch velocity calculations for "wild" flyrock since the launch velocity is one of the most important input parameters. The establishment of the valid and non-site-specific method for flyrock launch velocity prediction would allow wider use of the ballistic approach and our further research is developing in that direction.

The calculated distances of maximum throw are in fact the boundary of the impact zone and safe distance should be set at a larger distance according to the factor of safety. However, if the blast is conducted according to regulations and as designed, the "wild" flyrock has low probability of appearance, and the suggestion is to perform a risk assessment in order to define the risk zones within the impact zone. In the specific case of Kamenica quarry, the solution is to evacuate the residents of the nearest structures at every future blast and alert the residents of other surrounding structures. Also, considering the proximity of the primary school, the future blasts should be conducted on no school days or after school hours.

Acknowledgments

The authors of the paper thank Josip Cumin from Mechanical engineering faculty, University of Osjek, Croatia, for his contribution in providing the source code for the Runge–Kutta algorithm.

Appendix A. Supplementary materials

Supplementary materials associated with this article can be found in the online version at doi:10.1016/j.ijrmms.2011.07.004.

References

[1] Lundborg N. The probability of flyrock. Report DS.1981:5. Swedish Detonic Research Foundation, Stockholm; 1981. 39 p.
[2] Person PA, Holmberg R, Lee J Flyrock. In: Rock blasting and explosives engineering. Boca Raton: CRC Press; 1994. p. 319–35.
[3] Little TN. Flyrock risk. In: Proceedings of the EXPLO. Wollongong, Australasian Institute of Mining and Metallurgy; 2007. p. 35–43.
[4] Saunderson HS. Equations of motion and ballistic paths of volcanic ejecta. Comp Geosci 2008;34(7):802–14.
[5] Cumin J, Grizelj B, Scitovski R. Numerical solving of ballistic flight equations for big bore air rifle. Tech Gazette 2009;16(1):41–6.
[6] Coriolis effect. URL: 〈http://abyss.uoregon.edu/~js/glossary/coriolis_effect.html〉; [17.06.2011].
[7] Banchoff T, Chern SS, Pohl W. Differential geometry of curves and surfaces. New York: Springer; 2003.
[8] Dietz D, Iseri H. Calculus and differential geometry: an introduction to curvature. Dept Math Comp Info Sci, Mansfield University. URL: 〈http://faculty.mansfield.edu/hiseri/book-cdg.pdf〉; [17.06.2011].
[9] Mathews JH, Fink KK. Solution of differential equations, Runge Kutta methods. Numerical methods using Matlab.4th ed. New Jersey: Prentice-Hall; 2004. p. 489–96.
[10] Butcher JC. Numerical differential equation methods. numerical methods for ordinary differential equations.2nd ed. Chichester: Wiley; 2008. p. 51–136.
[11] Pantovic R, Zikic M, Stojadinovic S. A study on flyrock causes during blasting on Kamenica quarry. Invest Rep, Tech Fac Bor, Bor, Serbia; 2007 [Studija o uzrocima razletanja kamenih komada pri miniranju na PK Kamenica].
[12] NASA. Shape effect on drag. URL: 〈http://www.grc.nasa.gov/WWW/K-12/airplane/shaped.html〉; [17.06.2011].